Research Square

Preprints are preliminary reports that have not undergone peer review.
They should not be considered conclusive, used to inform clinical practice,
or referenced by the media as validated information.

Lumbar Vacuum Phenotypes in Degenerative Spondylolisthesis: Distinct Instability Signatures of Intradiscal and Facet Joint Gas

Xianyi Zhang
Second Affiliated Hospital of Xuzhou Medical College
QiRui Zhu
Second Affiliated Hospital of Xuzhou Medical College
Tianci Fang
Xuzhou Central Hospital
Jie Shang
Xuzhou Central Hospital
Lei Liu
Xuzhou Central Hospital
Guizhu Ji
Ruihua Affiliated Hospital of Soochow University
Ziwei Xia
Xuzhou Central Hospital
Youdi Xue
Xuzhou Central Hospital
Hengcai Zhou
Xuzhou Central Hospital
Meng Han
Xuzhou Central Hospital
Chao Ma
mc200866@126.com

Xuzhou Central Hospital

Article

Keywords: degenerative lumbar spondylolisthesis, intradiscal vacuum phenomenon, facet joint vacuum phenomenon, paraspinal muscle degeneration, dynamic radiograph, spinal instability

Posted Date: July 16th, 2026

DOI: https://doi.org/10.21203/rs.3.rs-10253584/v1

License: This work is licensed under a Creative Commons Attribution 4.0 International License.
Read Full License

Additional Declarations: No competing interests reported.

Abstract

Vacuum phenomenon (VP) is common in degenerative lumbar spondylolisthesis (DLS), but intradiscal and facet joint gas may represent different mechanical phenotypes. This retrospective CT-MRI dynamic radiograph study included 548 patients with single-level DLS classified as no VP (n = 184), isolated intradiscal VP (IDVP; n = 144), isolated facet joint VP (FJVP; n = 122), or combined VP (n = 98). Disc and facet degeneration, paraspinal muscle morphology, spinopelvic alignment, and flexion-extension parameters were compared, and multivariable logistic regression identified factors associated with IDVP and FJVP. Isolated IDVP showed greater disc height loss and higher Pfirrmann grades, whereas isolated FJVP showed more severe facet degeneration, facet effusion, and angular motion. Combined VP showed the greatest slippage, flexion-extension translation, PI-LL mismatch, and multifidus degeneration. Decreased disc height and higher Pfirrmann grade were independently associated with IDVP, while facet degeneration, moderate/severe effusion, angular motion, lower multifidus relative functional cross-sectional area, and PI-LL mismatch were independently associated with FJVP. IDVP and FJVP appear to represent overlapping but distinct anterior- and posterior-column instability signatures. VP phenotyping may provide a practical imaging framework for DLS risk stratification and future outcome-based studies.

Introduction

Degenerative lumbar spondylolisthesis (DLS) is a common degenerative spinal disorder characterized by anterior translation of a vertebral body without a pars interarticularis defect. Its development involves a complex interaction among disc degeneration, facet joint osteoarthritis, ligamentous laxity, sagittal spinopelvic morphology, and deterioration of the paraspinal dynamic stabilizers [1–3]. Because treatment decisions in DLS depend heavily on whether a segment is stable or unstable, identifying reliable imaging markers of instability remains clinically important.

The vacuum phenomenon (VP) refers to gas accumulation, composed predominantly of nitrogen, within a degenerated joint or disc space [4, 5]. In the lumbar spine, VP is most commonly observed within the intervertebral disc (intradiscal vacuum phenomenon, IDVP) but may also occur within the facet joint (facet joint vacuum phenomenon, FJVP). Since the early description of FJVP as a computed tomographic sign of degenerative spondylolisthesis, FJVP has been interpreted as a potential marker of posterior column degeneration and segmental hypermobility [6, 7]. However, IDVP and FJVP are frequently pooled together as a single degenerative sign, although their anatomical locations and biomechanical implications are fundamentally different.

IDVP is generally considered a sign of advanced disc degeneration, disc cavitation, and loss of disc height. Several studies have linked IDVP to vertical instability, altered disc-endplate loading, and worse clinical or mechanical outcomes after lumbar surgery [8–11]. In contrast, FJVP originates from gas accumulation within the facet joint capsule and may indicate capsular laxity, facet joint distraction, rotatory translation, or posterior column failure. Recent evidence suggests that intrafacet VP, rather than

intradiscal VP alone, may be particularly relevant to mechanical complications and adjacent segment disease after lumbar fusion [12].

Paraspinal muscles are central to the dynamic stabilization of the lumbar spine. The multifidus is a segmental stabilizer innervated by the medial branch of the dorsal ramus and is highly sensitive to abnormal segmental motion. Quantitative MRI studies have demonstrated that reduced functional muscle volume and increased fatty infiltration are associated with DLS severity, disc degeneration, and impaired postoperative recovery [13–16]. Whether different VP phenotypes are associated with distinct patterns of paraspinal muscle degeneration has not been fully clarified.

Previous studies have usually evaluated VP as a single binary imaging marker, whereas few have systematically distinguished IDVP from FJVP in relation to dynamic radiographic instability and paraspinal muscle degeneration. The three-joint complex was defined as the motion segment composed of the intervertebral disc and paired facet joints. Our hypothesis was that IDVP and FJVP represent predominant but overlapping instability phenotypes in DLS: IDVP reflecting an anterior column/disc-collapse phenotype, FJVP reflecting a posterior column/facet-instability phenotype, and combined VP reflecting global three-joint complex decompensation. To test this hypothesis, we performed a CT-MRI dynamic radiograph study in 548 patients with single-level DLS and compared structural, dynamic, spinopelvic, and paraspinal muscle parameters across four VP phenotypes.

Materials and Methods

Study hypothesis

We hypothesized that IDVP and FJVP would represent predominant but overlapping instability phenotypes in DLS: IDVP primarily reflecting anterior-column disc collapse and FJVP primarily reflecting posterior-column facet dysfunction, rotatory instability and local dynamic stabilizer degeneration.

Study design and participants

This single-center retrospective observational study was conducted at a tertiary spine center. The study was conducted in accordance with the Declaration of Helsinki and was reported according to the Strengthening the Reporting of Observational Studies in Epidemiology (STROBE) recommendations for observational studies [22]. The study protocol was approved by the Ethics Committee of Xuzhou Central Hospital (approval number: XZXY-LK-20230910-0121). The requirement for informed consent was waived by the ethics committee because all data were retrospectively collected and anonymized.

We reviewed consecutive patients diagnosed with single-level DLS between March 2018 and May 2023. Inclusion criteria were: (1) age 40 years or older; (2) radiographic diagnosis of single-level DLS; (3) Meyerding grade I or II spondylolisthesis; and (4) complete preoperative imaging, including lumbar CT, lumbar MRI, and standing flexion-extension lateral radiographs. Because DLS is uncommon in patients

younger than 40 years, this lower age limit was selected to reduce the likelihood of including non-degenerative etiologies. Exclusion criteria were: isthmic, traumatic, congenital, or pathological spondylolisthesis; multilevel DLS; Meyerding grade III or higher; previous lumbar surgery; spinal infection, tumor, fracture, or inflammatory spondyloarthropathy; neuromuscular disease affecting the paraspinal muscles; and incomplete or poor-quality imaging.

Imaging assessment

Lumbar CT was performed using a **64-slice multidetector CT scanner (Siemens Somatom Definition AS, Siemens Healthineers, Erlangen, Germany)** with the following parameters: tube voltage 120 kVp, tube current 200–300 mAs, slice thickness 1.0 mm, slice interval 0.5 mm, and bone kernel reconstruction. IDVP was defined as a well-demarcated gas-density area within the intervertebral disc space on axial or sagittal CT images. To improve diagnostic specificity and reduce partial-volume misclassification of fat or sclerosis, a unified threshold of ≤ -500 HU was used to define gas-density VP for both intradiscal and intrafacet locations [21]. FJVP was defined as a well-demarcated gas-density area within the facet joint space on axial CT images. The maximum width of facet gas was measured on the axial image showing the largest gas collection.

Facet joint degeneration was graded using the Weishaupt grading system based on joint space narrowing, osteophytes, subchondral sclerosis, and subchondral cysts [8]. Disc degeneration was graded according to the Pfirrmann classification on T2-weighted MRI [7]. Disc height was calculated as the mean of anterior, middle, and posterior disc heights on sagittal CT or MRI images; the middle disc height was measured at the midpoint between the adjacent vertebral endplates.

Lumbar MRI was performed using a **3.0T superconducting MRI system (Siemens Magnetom Skyra, Siemens Healthineers, Erlangen, Germany)** with a phased-array spine coil. The imaging protocol included:

Sagittal T1-weighted spin-echo sequence

TR/TE = 500/12 ms, slice thickness 4 mm, gap 0.4 mm

Sagittal T2-weighted fast spin-echo sequence

TR/TE = 3000/90 ms, slice thickness 4 mm, gap 0.4 mm

Axial T2-weighted fast spin-echo sequence

TR/TE = 2500/85 ms, slice thickness 3 mm, gap 0.3 mm

Axial T2-weighted fat-suppressed sequence

TR/TE = 2800/80 ms, slice thickness 3 mm, gap 0.3 mm

On axial T2-weighted images at the mid-disc level of the spondylolisthesis segment, or on the axial slice showing the largest disc area at the index level when the slipped segment made the level ambiguous, the multifidus and erector spinae were manually segmented using ImageJ software (version 1.54v, National Institutes of Health, Bethesda, MD, USA). Total cross-sectional area, fat area, and functional cross-sectional area (fCSA) were obtained. The relative functional cross-sectional area (rfCSA) was calculated as muscle fCSA divided by the vertebral body cross-sectional area at the same level. Fatty infiltration (FI) was calculated as fat area divided by total muscle area × 100%. In addition, multifidus fatty degeneration was qualitatively assessed according to the Goutallier grading system (grades 0-IV) based on the proportion of intramuscular fatty streaks [20]. Psoas muscle index (PMI) was measured at L3 and normalized by height squared. Facet joint effusion was graded as absent, mild, moderate, or severe according to the hyperintense fluid cleft on T2-weighted images. Ligamentum flavum thickness was measured at the facet joint level.

Bone mineral density (BMD) was measured using quantitative CT (QCT) at the L1-L3 vertebral bodies on the same CT examination. The average T-score of L1-L3 was calculated, and osteoporosis was defined as a T-score ≤ -2.5 standard deviations.

Standing neutral, flexion, and extension lateral radiographs were used to measure slippage percentage, flexion-extension translation, and angular motion. Slippage percentage was calculated as the anterior displacement of the slipped vertebra divided by the anteroposterior diameter of the caudal vertebral superior endplate × 100%. Flexion-extension translation was defined as the absolute change in slippage percentage between flexion and extension. Angular motion was defined as the absolute difference in the intervertebral Cobb angle between flexion and extension. Lumbar lordosis (LL), pelvic incidence (PI), pelvic tilt (PT), and sacral slope (SS) were measured on standing neutral lateral radiographs using standard Cobb methods; LL was measured from the upper endplate of L1 to the upper endplate of S1. Translation and angular motion were interpreted as dynamic surrogates of translational and rotational instability, respectively.

Phenotype classification

According to the presence of IDVP and/or FJVP on CT, patients were classified into four mutually exclusive phenotypes: no VP, isolated IDVP, isolated FJVP, and combined VP. Two senior spine surgeons independently assessed all images while blinded to clinical data. Disagreements were resolved by consensus with a senior spine specialist. Intra- and interobserver agreement was excellent for VP classification (IDVP kappa = 0.86, 95% CI: 0.81–0.91; FJVP kappa = 0.82, 95% CI: 0.76–0.88) and for continuous imaging measurements (ICC range: 0.85–0.92).

Sample size and power

Because this was a retrospective study of consecutive eligible patients, no formal a priori sample-size calculation was performed. A post hoc power assessment indicated that the final cohort of 548 patients provided more than 90% power to detect an odds ratio of 2.0 for the primary associations between VP phenotypes and key imaging predictors at a two-sided alpha level of 0.05, assuming an exposure prevalence of approximately 25%.

Statistical analysis

Continuous variables were tested for normality using the Shapiro-Wilk test and expressed as mean ± standard deviation or median with interquartile range, as appropriate. Categorical variables were expressed as number and percentage. Between-group comparisons were performed using one-way analysis of variance for normally distributed variables, Kruskal-Wallis tests for non-normally distributed variables, and chi-square or Fisher exact tests for categorical variables. Pairwise post hoc comparisons were adjusted for multiple testing using Tukey or Bonferroni correction; when variance heterogeneity was present, Welch analysis of variance with Games-Howell post hoc testing was used as a sensitivity approach.

Two multivariable logistic regression models were constructed to identify factors independently associated with IDVP and FJVP. Variables with $P < 0.10$ in univariable analysis and clinically relevant variables were considered for multivariable analysis. Multicollinearity was assessed using variance inflation factors, and variables with VIF < 5 were considered acceptable. Model calibration was assessed using the Hosmer-Lemeshow goodness-of-fit test. Odds ratios (ORs) with 95% confidence intervals (CIs) were reported. A two-sided $P < 0.05$ was considered statistically significant. Statistical analyses were performed using **SPSS version 26.0 (IBM Corp., Armonk, NY, USA)** and **R version 4.3.0 or later (R Foundation for Statistical Computing, Vienna, Austria)**.

Results

Patient characteristics and phenotype distribution

Figure 1 illustrates the patient selection process and vacuum phenotype distribution. Of 876 consecutive patients screened for eligibility, 328 were excluded because of multilevel DLS, Meyerding grade III or higher, previous lumbar surgery, incomplete imaging, or other exclusion criteria. A total of 548 patients with single-level DLS were included. The VP phenotype distribution was as follows: no VP in 184 patients (33.6%), isolated IDVP in 144 (26.3%), isolated FJVP in 122 (22.3%), and combined VP in 98 (17.9%). Baseline demographic variables were generally comparable among the four groups, including age, sex, BMI, disease duration, affected level, Meyerding grade, BMD T-score, diabetes mellitus, and smoking history. Low back pain VAS differed among groups ($P = 0.012$), and the combined VP group had a significantly higher VAS score than the no-VP group after multiplicity adjustment (adjusted $P = 0.008$; Table 1).

Table 1
Baseline characteristics according to VP phenotype.

Variable	No VP (n = 184)	Isolated IDVP (n = 144)	Isolated FJVP (n = 122)	Combined VP (n = 98)	P value
Age (years)	58.4 ± 8.2	60.1 ± 7.9	59.7 ± 8.5	61.3 ± 7.6	0.058
Female sex, n (%)	126 (68.5)	102 (70.8)	86 (70.5)	72 (73.5)	0.852
BMI (kg/m²)	26.8 ± 3.2	27.2 ± 3.5	27.5 ± 3.4	28.1 ± 3.1	0.062
Disease duration (months)	24.5 ± 18.2	26.8 ± 19.5	25.9 ± 17.8	28.3 ± 20.1	0.345
Affected level, n (%)					0.523
L3-L4	28 (15.2)	20 (13.9)	18 (14.8)	12 (12.2)	
L4-L5	112 (60.9)	92 (63.9)	76 (62.3)	64 (65.3)	
L5-S1	44 (23.9)	32 (22.2)	28 (23.0)	22 (22.4)	
Meyerding grade, n (%)					0.234
Grade I	128 (69.6)	94 (65.3)	80 (65.6)	58 (59.2)	
Grade II	56 (30.4)	50 (34.7)	42 (34.4)	40 (40.8)	
BMD T-score	-1.24 ± 0.85	-1.38 ± 0.92	-1.32 ± 0.88	-1.45 ± 0.95	0.215
Osteoporosis, n (%)	32 (17.4)	30 (20.8)	24 (19.7)	22 (22.4)	0.678
Diabetes mellitus, n (%)	28 (15.2)	26 (18.1)	22 (18.0)	20 (20.4)	0.654
Smoking history, n (%)	36 (19.6)	28 (19.4)	26 (21.3)	22 (22.4)	0.923
Low back pain VAS (score)	5.2 ± 1.8	5.6 ± 1.7	5.8 ± 1.9	6.1 ± 1.6	0.012

Values are mean ± standard deviation or number (%). BMI, body mass index; BMD, bone mineral density; FJVP, facet joint vacuum phenomenon; IDVP, intradiscal vacuum phenomenon; VAS, visual analogue scale; VP, vacuum phenomenon.

Disc- and facet-dominant structural phenotypes

CT and MRI structural parameters differed substantially across VP phenotypes (Table 2, Fig. 2, and Supplementary Fig. S1). Disc height was significantly lower in the isolated IDVP and combined VP groups than in the no-VP and isolated-FJVP groups after multiplicity-adjusted pairwise comparison. Pfirrmann grade distribution was also shifted toward more advanced disc degeneration in the IDVP-containing phenotypes. In contrast, facet degeneration was more severe in the isolated FJVP and

combined VP groups than in the no-VP and isolated-IDVP groups. The mean FJVP width was greater in the combined VP group than in the isolated FJVP group.

Table 2
CT and MRI structural degeneration parameters.

Variable	No VP (n = 184)	Isolated IDVP (n = 144)	Isolated FJVP (n = 122)	Combined VP (n = 98)	P value
Disc height (mm)	9.76 ± 2.05	6.12 ± 1.78[a][b]	8.94 ± 2.12[a]	5.86 ± 1.65[a][b]	< 0.001*
Pfirrmann grade, n (%)					< 0.001*
Grade II	24 (13.0)	6 (4.2)	18 (14.8)	2 (2.0)	
Grade III	86 (46.7)	42 (29.2)	56 (45.9)	22 (22.4)	
Grade IV	58 (31.5)	68 (47.2)	36 (29.5)	46 (46.9)	
Grade V	16 (8.7)	28 (19.4)	12 (9.8)	28 (28.6)	
Facet degeneration grade, n (%)					< 0.001*
Grade 0	22 (12.0)	18 (12.5)	6 (4.9)	2 (2.0)	
Grade 1	76 (41.3)	58 (40.3)	32 (26.2)	14 (14.3)	
Grade 2	62 (33.7)	48 (33.3)	52 (42.6)	36 (36.7)	
Grade 3	24 (13.0)	20 (13.9)	32 (26.2)	46 (46.9)	
FJVP width (mm)	-	-	1.86 ± 0.62	2.54 ± 0.78[d]	< 0.001*
Bilateral FJVP, n (%)	-	-	48 (39.3)	62 (63.3)[d]	0.001*

Facet degeneration was graded using the Weishaupt system. FJVP width was measured only in groups with FJVP; dashes indicate not applicable because no facet gas was present. VP was defined using a unified CT attenuation threshold of ≤ -500 HU. Superscripts indicate significant adjusted pairwise differences: a, vs. no VP; b, vs. isolated FJVP for IDVP-containing comparisons where applicable; c, vs. no VP; d, isolated FJVP vs. combined VP among FJVP-positive groups. FJVP, facet joint vacuum phenomenon; IDVP, intradiscal vacuum phenomenon; VP, vacuum phenomenon.

Paraspinal muscle and posterior element changes

Multifidus rfCSA decreased and multifidus FI increased in a stepwise pattern from no VP to isolated IDVP, isolated FJVP, and combined VP (Table 3 and Supplementary Fig. S2). Multiplicity-adjusted post hoc comparisons confirmed that the combined VP group had significantly lower multifidus rfCSA and higher FI than the other phenotypes (all adjusted $P < 0.05$). The proportion of severe multifidus fatty

degeneration (Goutallier grade 3/4) increased from 15.2% in the no-VP group to 49.0% in the combined VP group, supporting a graded posterior dynamic stabilizer failure pattern. Facet effusion and ligamentum flavum thickness were also greatest in the FJVP-containing phenotypes, particularly the combined VP group. PMI differed only modestly among groups, suggesting that posterior paraspinal muscle degeneration was more phenotype-specific than psoas morphology.

Table 3
Paraspinal muscle and posterior element parameters.

Variable	No VP (n = 184)	Isolated IDVP (n = 144)	Isolated FJVP (n = 122)	Combined VP (n = 98)	P value
Multifidus rfCSA	0.856 ± 0.134	0.768 ± 0.125□	0.712 ± 0.118□□	0.624 ± 0.112□□□	< 0.001*
Multifidus FI (%)	22.35 ± 6.42	28.64 ± 7.23□	32.45 ± 7.86□□	39.24 ± 8.65□□□	< 0.001*
Goutallier grade, n (%)					< 0.001*
Grade 0	28 (15.2)	14 (9.7)	8 (6.6)	2 (2.0)	
Grade 1	72 (39.1)	48 (33.3)	32 (26.2)	16 (16.3)	
Grade 2	56 (30.4)	52 (36.1)	48 (39.3)	32 (32.7)	
Grade 3	22 (12.0)	24 (16.7)	26 (21.3)	34 (34.7)	
Grade 4	6 (3.3)	6 (4.2)	8 (6.6)	14 (14.3)	
Erector spinae rfCSA	0.724 ± 0.112	0.685 ± 0.108	0.656 ± 0.105	0.598 ± 0.098	< 0.001*
PMI (cm^2/m^2)	5.86 ± 1.24	5.68 ± 1.18	5.72 ± 1.22	5.54 ± 1.15	0.186
Facet effusion grade, n (%)					< 0.001*
Absent	86 (46.7)	62 (43.1)	28 (23.0)	12 (12.2)	
Mild	68 (37.0)	52 (36.1)	46 (37.7)	28 (28.6)	
Moderate	24 (13.0)	22 (15.3)	34 (27.9)	38 (38.8)	
Severe	6 (3.3)	8 (5.6)	14 (11.5)	20 (20.4)	
Moderate/severe effusion, n (%)	30 (16.3)	30 (20.8)	48 (39.3)	58 (59.2)	< 0.001*
Ligamentum flavum thickness (mm)	3.24 ± 0.68	3.56 ± 0.72	3.88 ± 0.75	4.26 ± 0.82	< 0.001*

Goutallier grade is a qualitative ordinal grading system for fatty muscle degeneration, whereas FI and rfCSA are quantitative MRI-derived parameters. Superscripts indicate significant adjusted pairwise differences: a, vs. no VP; b, vs. isolated IDVP; c, vs. isolated FJVP. FI, fatty infiltration; PMI, psoas muscle index; rfCSA, relative functional cross-sectional area. *P < 0.05 indicates statistical significance.

Dynamic radiographic instability

Dynamic radiographic parameters demonstrated predominant but overlapping instability signatures (Table 4 and Supplementary Fig. S3). Isolated IDVP was associated with increased slippage percentage and translation compared with no VP, consistent with disc-collapse-related instability. Isolated FJVP was associated with greater angular motion than isolated IDVP, supporting a posterior column or rotatory instability phenotype. The combined VP group had the highest slippage percentage and largest flexion-extension translation, suggesting global instability of the three-joint complex. In addition, PI-LL mismatch differed significantly across phenotypes and reached its highest value in the combined VP group (Table 4).

Table 4
Dynamic radiographic and spinopelvic parameters.

Variable	No VP (n = 184)	Isolated IDVP (n = 144)	Isolated FJVP (n = 122)	Combined VP (n = 98)	P value
Slippage percentage (%)	12.35 ± 4.12	15.68 ± 4.85[a]	14.26 ± 4.52	18.64 ± 5.23[a,b,c]	< 0.001*
Flexion-extension translation (%)	4.25 ± 1.56	6.12 ± 1.89[a]	5.68 ± 1.76[a]	8.34 ± 2.15[a,b,c]	< 0.001*
Angular motion (°)	4.86 ± 1.72	5.16 ± 1.89	7.82 ± 2.34[a,b]	9.24 ± 2.56[a,b,c]	< 0.001*
LL (°)	42.5 ± 8.6	40.8 ± 9.2	41.2 ± 8.8	39.6 ± 9.5	0.156
PI (°)	52.4 ± 10.2	53.6 ± 11.5	51.8 ± 10.8	54.2 ± 11.2	0.342
PT (°)	18.6 ± 5.8	19.2 ± 6.2	18.8 ± 5.6	20.4 ± 6.5	0.189
SS (°)	33.8 ± 7.2	34.4 ± 7.8	33.0 ± 7.5	33.8 ± 8.1	0.567
PI-LL mismatch (°)	9.9 ± 6.8	12.8 ± 7.5	10.6 ± 7.2	14.6 ± 8.2	0.002*

Dynamic parameters were measured from standing flexion-extension lateral radiographs. Slippage percentage was calculated as anterior displacement divided by the anteroposterior diameter of the caudal vertebral superior endplate × 100%; angular motion was the absolute flexion-extension change in intervertebral Cobb angle. Superscripts indicate significant adjusted pairwise differences: a, vs. no VP; b, vs. isolated IDVP; c, vs. isolated FJVP. LL, lumbar lordosis; PI, pelvic incidence; PI-LL mismatch, pelvic incidence minus lumbar lordosis mismatch; PT, pelvic tilt; SS, sacral slope.

Multivariable regression analyses

In multivariable analysis, decreased disc height, higher Pfirrmann grade, slippage percentage, and PI-LL mismatch were independently associated with IDVP, whereas facet degeneration grade, moderate/severe facet effusion, angular motion, lower multifidus rfCSA, PI-LL mismatch, older age, and higher BMI were independently associated with FJVP (Table 5 and Fig. 3). Angular motion showed a near-significant association in the IDVP model, supporting the interpretation that IDVP- and FJVP-related instability mechanisms are predominant rather than fully mutually exclusive. Complete univariable regression results are provided in Supplementary Table S1.

The Hosmer-Lemeshow goodness-of-fit test indicated good calibration for both models. The IDVP model showed χ^2=6.23 (df = 8, P = 0.621) with a C-statistic of 0.782 (95% CI: 0.734–0.830), and the FJVP model showed χ^2=5.87 (df = 8, P = 0.662) with a C-statistic of 0.815 (95% CI: 0.772–0.858).

All variance inflation factors were below 3.5, indicating no significant multicollinearity among variables retained in the final models.

Table 5
Multivariable logistic regression analyses for IDVP and FJVP.

Variable	IDVP model			FJVP model		
	OR (95% CI)	P value	VIF	OR (95% CI)	P value	VIF
Age (per 5-year increase)	1.124 (0.956–1.321)	0.156	1.24	1.235 (1.045–1.460)	0.013	1.28
BMI (per 1 kg/m² increase)	1.056 (0.978–1.140)	0.168	1.18	1.124 (1.032–1.225)	0.008	1.22
Disc height (per 1 mm decrease)	3.245 (2.156–4.887)	< 0.001	2.56	1.156 (0.789–1.692)	0.456	2.34
Pfirrmann grade (per grade increase)	2.156 (1.543–3.012)	< 0.001	2.34	1.345 (0.987–1.832)	0.062	2.15
Facet degeneration grade (per grade increase)	1.124 (0.856–1.476)	0.398	2.12	2.876 (2.015–4.105)	< 0.001	2.45
Moderate/severe facet effusion	1.345 (0.876–2.065)	0.178	1.89	4.128 (2.876–5.923)	< 0.001	2.12
Slippage percentage (per 5% increase)	1.568 (1.123–2.189)	0.008	2.45	1.213 (0.945–1.557)	0.132	2.34
Angular motion (per 2° increase)	1.345 (0.978–1.852)	0.068	2.23	2.543 (1.765–3.667)	< 0.001	2.56
Multifidus rfCSA (per 0.1 decrease)	1.345 (0.956–1.892)	0.089	2.56	1.876 (1.287–2.734)	0.001	2.78
Ligamentum flavum thickness (per 1 mm increase)	1.156 (0.823–1.623)	0.402	1.98	1.345 (0.956–1.892)	0.089	2.05
PI-LL mismatch (per 5° increase)	1.345 (1.098–1.648)	0.005	1.76	1.234 (1.005–1.515)	0.045	1.88

Two separate logistic regression models were fitted. Multicollinearity was assessed before model entry, and model fit was checked using the Hosmer-Lemeshow goodness-of-fit test. The step size for rfCSA was set at 0.1 because this interval approximates the observed variability of this ratio and improves clinical interpretability of the OR. BMI, body mass index; CI, confidence interval; FJVP, facet joint vacuum

phenomenon; IDVP, intradiscal vacuum phenomenon; OR, odds ratio; PI-LL, pelvic incidence-lumbar lordosis; rfCSA, relative functional cross-sectional area; VIF, variance inflation factor.

Model performance:

IDVP model: C-statistic = 0.782 (95% CI: 0.734–0.830), Hosmer-Lemeshow χ^2 = 6.23, P = 0.621

FJVP model: C-statistic = 0.815 (95% CI: 0.772–0.858), Hosmer-Lemeshow χ^2 = 5.87, P = 0.662

Discussion

This CT, MRI and dynamic radiograph study demonstrates that IDVP and FJVP are not interchangeable CT signs in DLS. IDVP was mainly associated with disc height loss and advanced disc degeneration, whereas FJVP was more strongly associated with facet degeneration, facet effusion, angular motion and multifidus degeneration. Combined VP showed the most severe translational instability, PI-LL mismatch and posterior muscle degeneration. These findings support a phenotype-based interpretation of VP in which anterior-column disc collapse and posterior-column facet dysfunction are dominant but overlapping mechanisms rather than mutually exclusive disease entities.

Interpretation of VP Phenotypes

The IDVP phenotype is biologically consistent with disc cavitation. Progressive dehydration, annular fissuring and endplate-disc degeneration can reduce intradiscal pressure and permit gas accumulation within the disc space [4, 5, 21]. The independent associations of decreased disc height and higher Pfirrmann grade with IDVP support the view that IDVP primarily marks anterior column collapse. In clinical assessment, an IDVP-dominant segment should therefore prompt careful evaluation of foraminal height loss, discogenic mechanical pain and the potential need for disc-height restoration when fusion is otherwise indicated.

FJVP showed a distinct posterior-column profile. Its independent associations with facet degeneration, moderate/severe effusion and angular motion suggest that intra-articular facet gas reflects capsular laxity, facet distraction and rotatory instability [6, 9–12]. The strong relationship between FJVP and multifidus degeneration further supports a posterior-column instability mechanism because the multifidus directly stabilizes the facet-bearing motion segment.

Although facet degeneration, facet effusion and FJVP are anatomically related, they capture different pathological dimensions rather than a single redundant construct. In our multivariable model, all retained variables had variance inflation factors below 3.5, supporting acceptable independence among predictors. Facet degeneration reflects irreversible structural remodeling, including osteophytes, sclerosis and joint-space narrowing; effusion indicates synovial inflammation and capsular laxity with dynamic fluid accumulation; and FJVP represents gas filling under negative intra-articular pressure during capsular distraction. Therefore, the independent associations of facet degeneration and

moderate/severe effusion with FJVP should be interpreted as a progressive posterior-column cascade from structural damage to functional instability, rather than as tautology.

The combined VP phenotype probably represents global decompensation of the three-joint complex. These patients had the greatest slippage percentage, largest flexion-extension translation and highest PI-LL mismatch. The near-significant association between angular motion and IDVP in the IDVP model also suggests that disc-collapse and rotational components can coexist within the same segment. Therefore, VP phenotypes should be used to identify dominant instability signatures, not to force patients into rigid categories.

Spinopelvic Alignment and VP

PI-LL mismatch was independently associated with both IDVP and FJVP. This indicates that sagittal malalignment may act as a shared biomechanical background, increasing both anterior disc loading and posterior facet stress. In DLS, local VP should therefore be interpreted alongside global and regional alignment rather than as an isolated CT finding. This shared alignment factor further reinforces the concept that VP phenotypes exist on a continuum of global sagittal imbalance rather than as purely segmental disorders.

Paraspinal Muscle Degeneration and Instability

The stepwise deterioration of multifidus morphology across VP phenotypes is another key finding. Multifidus rfCSA was lowest and FI highest in the combined VP group, whereas PMI showed only modest differences. This pattern suggests a posterior-column-specific process rather than generalized sarcopenia alone. Recent evidence also supports close associations among facet degeneration, lumbar instability and multifidus fatty infiltration [16–19]. A plausible vicious cycle is that facet degeneration and abnormal micromotion promote multifidus inhibition or fatty replacement, while loss of multifidus functional volume further reduces segmental dynamic control.

Clinical Implications

These findings may refine DLS surgical planning. IDVP-dominant segments may require attention to disc collapse and foraminal height restoration when fusion is clinically justified. FJVP-dominant segments should raise concern for facet-mediated pain, angular instability and postoperative destabilization after wide posterior decompression. Combined VP may represent the highest-risk phenotype and should prompt careful evaluation of fusion or stabilization indications, especially when dynamic radiographs, PI-LL mismatch and multifidus degeneration are concordant. Because VP phenotypes can be evaluated on routine CT and combined with MRI-derived muscle metrics and dynamic radiographs, they may provide a practical framework for imaging-based risk stratification.

Future Directions

Separating IDVP and FJVP may reduce heterogeneity in future DLS research and may help explain why similar Meyerding grades can show different mechanical behavior. In outcome-based studies, VP

phenotypes should be tested against conservative-treatment response, decompression-alone failure, fusion outcomes, adjacent-segment degeneration and implant-related mechanical complications.

Limitations

Several limitations should be acknowledged. First, the retrospective single-center design limits causal inference and generalizability. Second, CT, MRI and dynamic radiographs were acquired in different positions, and supine CT may underestimate VP extent under physiologic loading. Third, this study focused on imaging phenotypes and did not include long-term surgical outcomes, fusion status, ODI or longitudinal pain trajectories. Fourth, although representative CT panels were added, three-dimensional gas-volume measurement was not performed. Fifth, residual confounding by occupational load, physical activity, metabolic status, osteoporosis severity and unmeasured neuromuscular factors cannot be excluded. Finally, the age cutoff of 40 years minimized non-degenerative etiologies, but sensitivity analyses using a higher cutoff would further test robustness.

Overall, iDVP and FJVP are dominant yet overlapping instability phenotypes in DLS. IDVP mainly reflects anterior-column disc collapse, whereas FJVP is linked to posterior facet dysfunction, angular instability and multifidus degeneration. Combined VP may indicate global three-joint complex decompensation. Integrating VP phenotype with dynamic radiographs, spinopelvic alignment and paraspinal muscle assessment may provide a practical imaging framework for DLS risk stratification and hypothesis generation for future outcome-based surgical studies. Prospective outcome-based validation is warranted.

Abbreviations

BMI
body mass index
BMD
bone mineral density
CI
confidence interval
CT
computed tomography
DLS
degenerative lumbar spondylolisthesis
FI
fatty infiltration
FJVP
facet joint vacuum phenomenon
HU
Hounsfield unit
ICC

intraclass correlation coefficient
IDVP
intradiscal vacuum phenomenon
LL
lumbar lordosis
MRI
magnetic resonance imaging
OR
odds ratio
PI
pelvic incidence
PMI
psoas muscle index
PT
pelvic tilt
QCT
quantitative computed tomography
rfCSA
relative functional cross-sectional area
SS
sacral slope
STROBE
Strengthening the Reporting of Observational Studies in Epidemiology
VAS
visual analogue scale
VP
vacuum phenomenon.

Declarations

Ethics approval and consent to participate

This study adhered to the ethical principles of the Declaration of Helsinki and was approved by the Biomedical Research Ethics Committee of Xuzhou Central Hospital (Approval No. XZXY-LK-20230910-0121

Consent for publication

Not applicable.

Competing interests

The authors declare no competing interests.

Funding statement

This study was supported by the Project of Xuzhou Municipal Health Commission (Grant No. KC21206), Contract for Science and Technology Projects of Xuzhou Health Commission (Grant No. XWKYHT20230054), Jiangsu Provincial Medical Center (Grant No. QNRC2016392), Pengcheng Talents - Medical Young Reserve Talents Training Project (Grant No. XWRCHT20220020), and Xuzhou Science and Technology Project Contract (Grant No. KC23177).

Author Contribution

X.Y.Z., Q.R.Z. and T.C.F. contributed equally to this work. X.Y.Z., Q.R.Z., T.C.F., M.H. and C.M. conceived and designed the study. X.Y.Z., Q.R.Z., T.C.F., J.S., L.L., G.Z.J., Z.W.X., Y.D.X. and H.C.Z. collected the clinical and imaging data. X.Y.Z., Q.R.Z., T.C.F., J.S. and G.Z.J. performed image assessment and data verification. X.Y.Z., Q.R.Z. and T.C.F. performed the statistical analyses and prepared the initial manuscript draft. J.S., L.L., Z.W.X., Y.D.X. and H.C.Z. assisted with data interpretation and manuscript revision. M.H. and C.M. supervised the study, provided methodological guidance, and critically revised the manuscript for important intellectual content. All authors reviewed and approved the final manuscript.

Acknowledgements

No acknowledgements to declare.

Data Availability

The datasets used and analyzed in this study can be obtained from the corresponding author upon reasonable request.

References

1. Rangwalla, K. et al. Degenerative lumbar spondylolisthesis: review of current classifications and proposal of a novel classification system. *Eur. Spine J.* **33**, 1701–1715. https://doi.org/10.1007/s00586-023-07818-x (2024).
2. Krenzlin, H. et al. Intermodal detection of lumbar instability in degenerative spondylolisthesis. *Front. Surg.* **9**, 860865. https://doi.org/10.3389/fsurg.2022.860865 (2022).
3. Cabrera, J. P. et al. What radiographic and spinopelvic parameters do spine surgeons consider in decision-making for treatment of degenerative lumbar spondylolisthesis? *Global Spine J.* **15**, 1717–

1727. https://doi.org/10.1177/21925682241306105 (2025).

4. Ford, L. T., Gilula, L. A., Murphy, W. A. & Gado, M. Analysis of gas in vacuum lumbar disc. *AJR Am. J. Roentgenol.* **128**, 1056–1057. https://doi.org/10.2214/ajr.128.6.1056 (1977).
5. Cawley, D. T. et al. Intra-discal vacuum phenomenon with advanced lumbar spine degeneration: an imaging characterization study. *J. Spine Surg.* **11**, 226–235. https://doi.org/10.21037/jss-2024-055 (2025).
6. Sun, Z. et al. Vacuum facet phenomenon in computed tomography imaging: a sign of instability in degenerative spondylolisthesis? *World Neurosurg.* **129**, e393–e400. https://doi.org/10.1016/j.wneu.2019.05.163 (2019).
7. Pfirrmann, C. W. A., Metzdorf, A., Zanetti, M., Hodler, J. & Boos, N. Magnetic resonance classification of lumbar intervertebral disc degeneration. *Spine* **26**, 1873–1878. https://doi.org/10.1097/00007632-200109010-00011 (2001).
8. Weishaupt, D., Zanetti, M., Boos, N. & Hodler, J. MR imaging and CT in osteoarthritis of the lumbar facet joints. *Skeletal Radiol.* **28**, 215–219. https://doi.org/10.1007/s002560050503 (1999).
9. Singh, K., Hislop, T., Lahiri, A. & Tekke, P. Lumbar facet joint fluid: a reliable sign of lumbar instability. Cureus 15, e39332 (2023). https://doi.org/10.7759/cureus.39332
10. Aggarwal, A. & Garg, K. Lumbar facet fluid: does it correlate with dynamic instability in degenerative spondylolisthesis? A systematic review and meta-analysis. *World Neurosurg.* **149**, 53–63. https://doi.org/10.1016/j.wneu.2021.02.029 (2021).
11. Elmose, S. F., Andersen, G. O., Carreon, L. Y., Sigmundsson, F. G. & Andersen, M. O. Radiological definitions of sagittal plane segmental instability in the degenerative lumbar spine: a systematic review. *Global Spine J.* **13**, 2426–2439. https://doi.org/10.1177/21925682221099854 (2023).
12. Kohli, P. et al. Facet vacuum phenomenon is associated with better clinical outcomes in case of fusion vs decompression alone for degenerative spondylolisthesis. *N Am. Spine Soc. J.* **18**, 100362. https://doi.org/10.1016/j.xnsj.2024.100362 (2024).
13. Camino-Willhuber, G. et al. Association between lumbar intervertebral vacuum phenomenon severity and posterior paraspinal muscle atrophy in patients undergoing spine surgery. *Eur. Spine J.* **33**, 1013–1020. https://doi.org/10.1007/s00586-023-08120-6 (2024).
14. Moradi, F., Bagheri, S. R., Ataee, M. & Alimohammadi, E. Can magnetic resonance imaging findings effectively diagnose the instability observed on radiographs in patients with degenerative lumbar spinal stenosis? *J. Orthop. Surg. Res.* **19**, 459. https://doi.org/10.1186/s13018-024-04963-x (2024).
15. Ozcan Eksi, E. E., Eksi, M. S., Karakas, F. & Celikoglu, E. Could alteration in the vacuum phenomenon rather than its presence be a sign of spinal instability? Eur. *Spine J.* **35**, 1723–1735. https://doi.org/10.1007/s00586-025-09198-w (2026).
16. Da, W. et al. Quantitative analysis of relationship between paraspinal muscle degeneration and degree of degenerative lumbar spondylolisthesis. *Spine* **50**, 1327–1335. https://doi.org/10.1097/BRS.0000000000005270 (2025).

17. Miki, T. et al. Associations between paraspinal muscle morphology, disc degeneration, and clinical features in patients with lumbar spinal stenosis. *Prog Rehabil Med.* **5**, 20200015. https://doi.org/10.2490/prm.20200015 (2020).
18. Han, G., Jiang, Y., Zhang, B., Gong, C. & Li, W. Imaging evaluation of fat infiltration in paraspinal muscles on MRI: a systematic review with a focus on methodology. *Orthop. Surg.* **13**, 1141–1148. https://doi.org/10.1111/os.12962 (2021).
19. Mardulyn, T., Delafontaine, A., Jissendi, P. & Fabeck, L. Lumbar muscle fatty infiltration and atrophy in patients with low back pain and degenerative spinal pathologies: a CT imaging study. *J. Clin. Med.* **14**, 2125. https://doi.org/10.3390/jcm14062125 (2025).
20. Goutallier, D., Postel, J. M., Bernageau, J., Lavau, L. & Voisin, M. C. Fatty muscle degeneration in cuff ruptures: pre- and postoperative evaluation by CT scan. *Clin. Orthop. Relat. Res.* **304**, 78–83 (1994).
21. Buttiens, A., Simko, M. & Van Goethem, J. Vacuum phenomenon in the lumbar spine: pilot study for accuracy of magnetic resonance imaging. *J. Belg. Soc. Radiol.* **107**, 83. https://doi.org/10.5334/jbsr.3118 (2023).
22. von Elm, E. et al. The Strengthening the Reporting of Observational Studies in Epidemiology (STROBE) statement: guidelines for reporting observational studies. *Lancet* **370**, 1453–1457. https://doi.org/10.1016/S0140-6736(07)61602-X (2007).

Figures

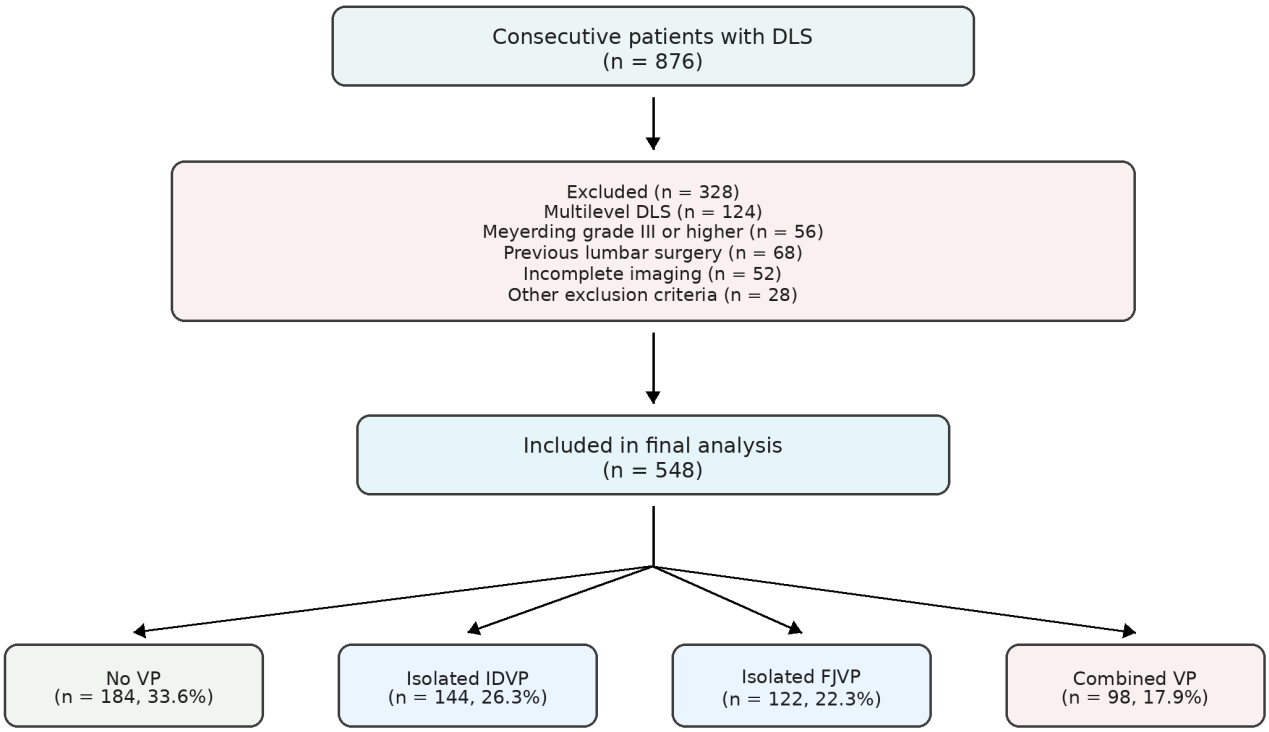


Figure 1

Patient selection and vacuum phenotype grouping. DLS, degenerative lumbar spondylolisthesis; FJVP, facet joint vacuum phenomenon; IDVP, intradiscal vacuum phenomenon; VP, vacuum phenomenon.

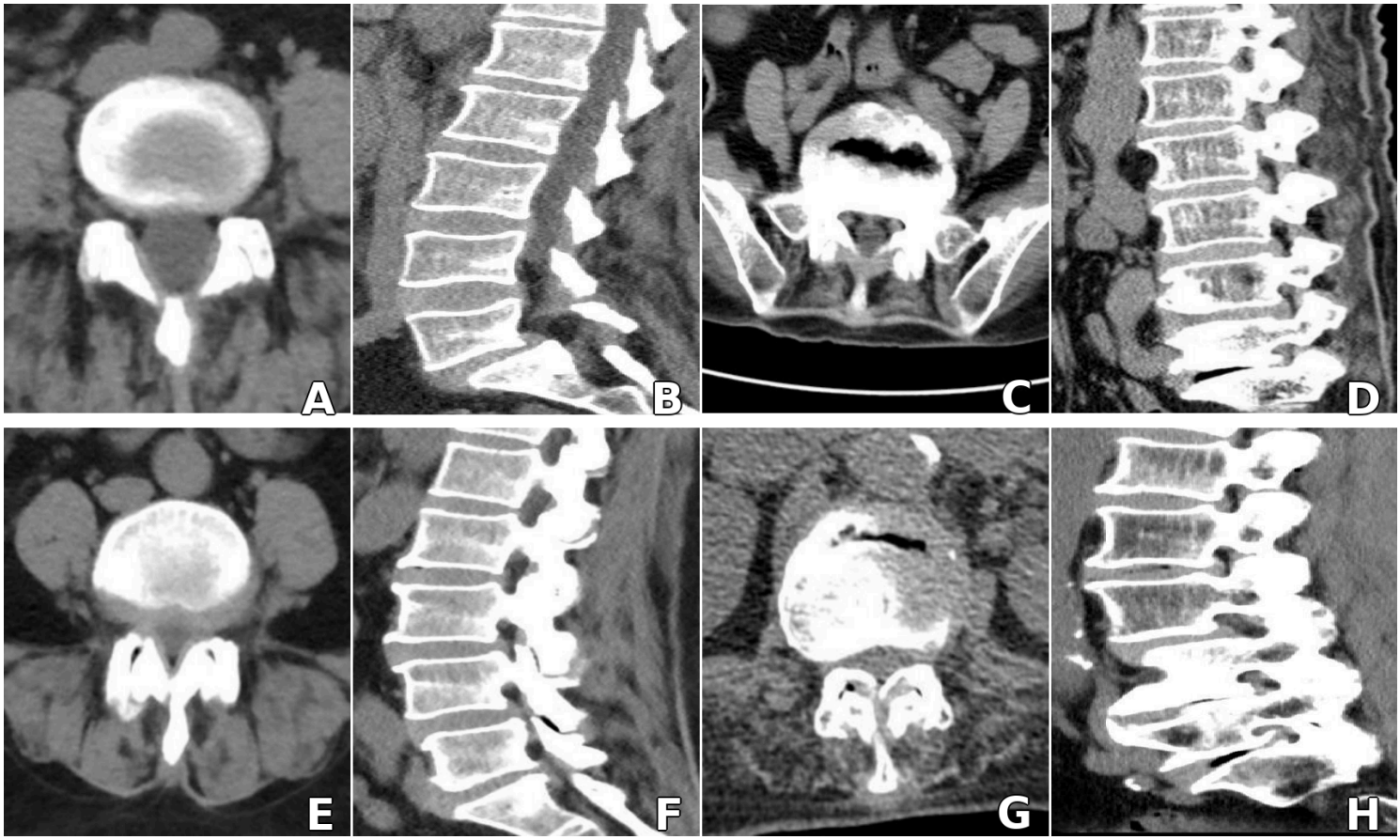


Figure 2

Representative anonymized CT images illustrating VP phenotypes. Panels A/B, C/D, E/F, and G/H show representative axial and sagittal CT examples of no VP, isolated IDVP, isolated FJVP, and combined VP, respectively. All panels were standardized to the same display size for radiological comparison. VP, vacuum phenomenon; IDVP, intradiscal vacuum phenomenon; FJVP, facet joint vacuum phenomenon.

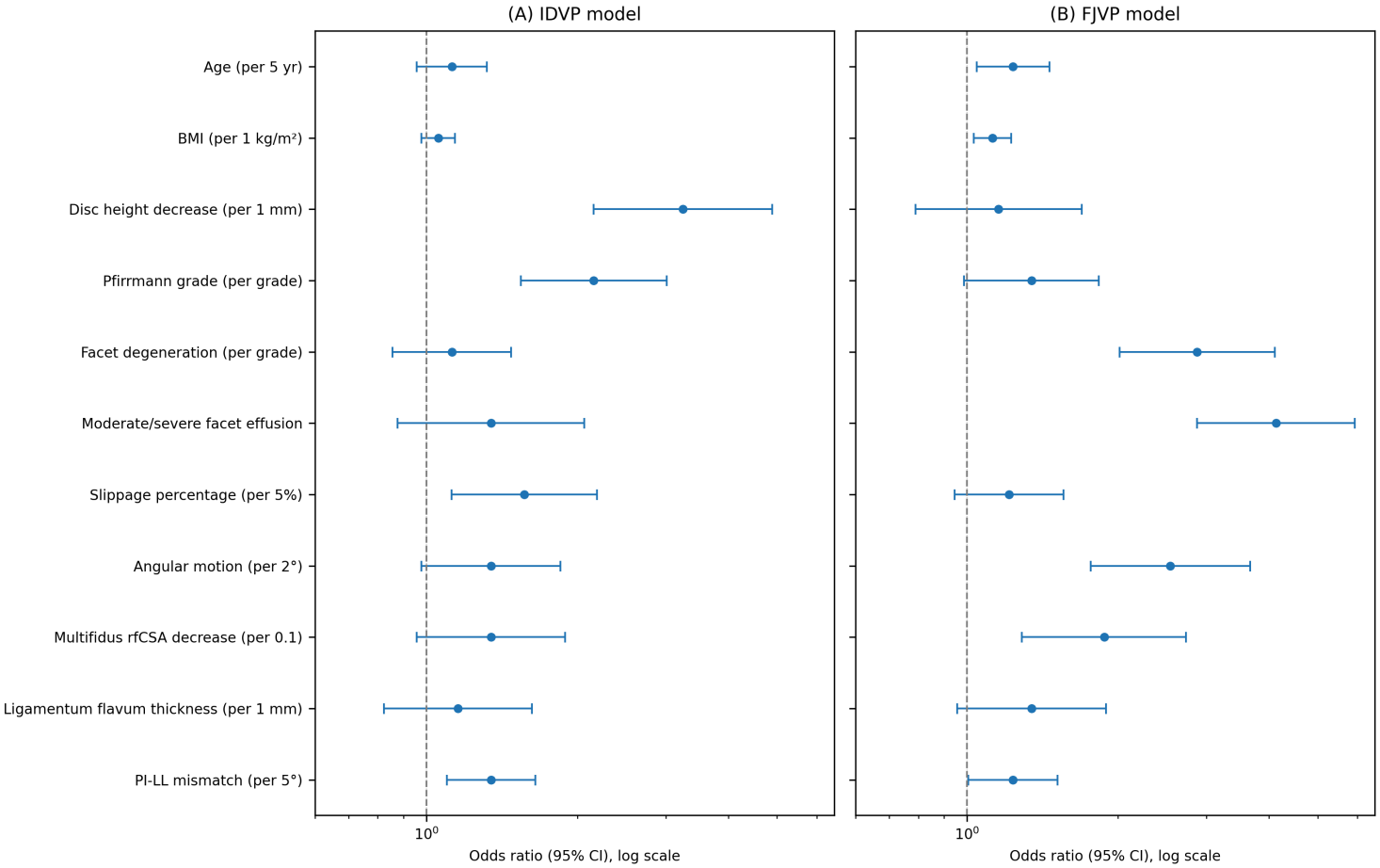


Figure 3

Forest plot of multivariable logistic regression models for IDVP and FJVP. (A) IDVP model. (B) FJVP model. ORs are plotted on a logarithmic scale; horizontal bars represent 95% CIs. BMI, body mass index; CI, confidence interval; FJVP, facet joint vacuum phenomenon; IDVP, intradiscal vacuum phenomenon; OR, odds ratio; PI-LL, pelvic incidence-lumbar lordosis; rfCSA, relative functional cross-sectional area.

Supplementary Files

This is a list of supplementary files associated with this preprint. Click to download.

- Supplementarymaterial.docx